Structures of Poly(2-hydroxy-6-naphthoic acid) at Ambient and High Temperatures

Pio Iannelli,*,† Do Y. Yoon,‡ and William Parrish‡

Dipartimento di Fisica, Università di Salerno, I-84081 Baronissi, Italy, and IBM Research Division, Almaden Research Center, 650 Harry Road, San Jose, California 95120-6099

Received November 12, 1993; Revised Manuscript Received February 3, 1994®

ABSTRACT: The structures of poly(2-hydroxy-6-naphthoic acid) (PHNA), $(C_{10}H_6COO)_x$, at room and high temperatures accompanying the phase transition at ca. 340 have been determined by X-ray powder diffraction analysis. The PHNA data at room temperature can be explained by an orthorhombic cell with a = 7.66 (1) Å, b = 5.98 (1) Å, and c = 17.12 (3) Å, space group $Pbc2_1$ (four $C_{10}H_6COO$ units, ρ_{calc} = 1.44 g cm^{-3}), and the naphthoic rings staggered by ca. 120° along the chain. Disorder has been considered in the packing by giving equal occupancy to the two molecules oriented *up* or *down* along the c cell axis and some degree of molecular mobility along the c axis. The space group $Iba2$ was found at 370 °C with the cell parameters a = 9.28 Å, b = 5.64 Å, and c = 17.04 Å (four $C_{10}H_6COO$, ρ_{calc} = 1.27 g cm^{-3}). The new structure can be explained starting from the room temperature one by applying a rotational statistical model involving a 2-fold axis around the chain axis, analogous to a smectic E phase.

Introduction

In the last few years much research has been conducted to characterize the structure and the properties of the copolymers of 4-hydroxybenzoic acid (HBA) and 2-hydroxy-6-naphthoic acid (HNA). Among these only a few publications concern the synthesis and characterization of the homopolymer poly(2-hydroxy-6-naphthoic acid) (PHNA).[1-4] These investigations have shown the analogy between the properties of PHNA and the homopolymer poly(4-hydroxybenzoic acid) (PHBA).[4,5] A similar thermal behavior, with two reversible transitions in the DSC trace, has been stressed. For PHNA, the two endotherms occurring at ca. 340 and ca. 440 °C have been interpreted as accompanying a crystal to plastic crystal transition and the melting to the nematic phase, respectively.[3] Kricheldorf *et al.* observed a third transition at ≈540 °C in the DSC trace of their needlelike crystals of PHNA.[4] They suggest the appearance of a rotatory phase at the second transition with the retention of the chain conformation. This residual order is lost at 540 °C.

The molecular structure of the phase stable at the high temperatures of PHBA has been already solved and discussed[6,7] in terms of a conformational model very much like that of a smectic-E phase of rodlike molecules.[6] No conformational and molecular packing analysis of the phase stable at room temperature of both PHNA and PHBA has been reported, as well as the structure model of the high-temperature phase of PHNA. In order to better understand the molecular structure of this class of stiff polymers and the structural modifications occurring at the first DSC transition, this paper deals with the molecular structure analysis of PHNA. The molecular structure of phases stable at room temperature of PHBA will be discussed in a separate paper.[8]

Experimental Section

PHNA was synthesized according to the procedure of ref 3. For conducting the X-ray diffraction measurements, all the specimens were prepared as a fine powder spread evenly on a 10 × 25 mm area of a thin silicon single-crystal wafer surface, cut parallel to the (510) plane (to minimize scattering from the substrate) using 5% collodion in amyl acetate as a binder. A vertical-scanning-type powder diffractometer operating in a standard θ–2θ geometry[9] and a standard copper target long line focus tube operated at 50 kV/25 mA were used. Beam collimation was provided by a 1.0° entrance slit to define the primary beam, an antiscatter slit, and a 0.12° receiving slit in the diffracted beam. Vertical divergence was limited by 4° Soller slits in the incident beam. A curved graphite monochromator was placed after the receiving slit to reflect only Cu Kα radiation. The data used for structure analysis were recorded with a counting time of 4 s and a 0.02° 2θ step size. The detector was a Na(Tl) I scintillation counter with pulse amplitude discrimination.

The high-temperature X-ray measurements were made in a high-temperature X-ray specimen chamber designed for polymer phase studies. The single-crystal wafer with powder on the top surface was mounted on a flat silicon nitride plate containing an internal electric heating element. A cylindrical heat shield with a long beryllium window fit over the heater and an outer vacuum-tight chamber with a Mylar window covered the assembly. The actual temperature of the specimen was measured with ±5 °C precision by a chromel–alumel thermocouple in contact with the silicon wafer and maintained by a digital temperature controller. The diffraction experiments were performed under low vacuum (0.5 Torr), in order to avoid air scatter and absorption losses and to prevent possible oxidation of the specimen.

Results and Discussion

PHNA at Room Temperature. The diffraction pattern of PHNA at room temperature is shown in Figure 1a. The specimen had been previously annealed at 280 °C for about 1 h. Thirteen peaks were clearly identified by means of a peak search program using the cubic first derivative method;[10] they were used in the indexing and unit cell determination. The data are listed in Table 1.

Since PHNA is not processable, no oriented samples could be prepared, thus limiting the structural analysis to the random powder diffraction method. Biswas et al.[11] used copolymers of HNA and HBA as a model of wholly aromatic polymers and investigated oriented fiber samples. They analyzed the X-ray diffraction data in terms of a phase with pseudoorthorhombic symmetry.

In the case of the homopolymer PHBA, electron diffraction studies were made[12] using tiny single crystals; the data were explained in terms of two phases both with orthorhombic cells. For poly(*p*-phenylene terephthalamide), Northolt[13] proposed a rectangular monoclinic cell (γ = 90°), probable space group Pn or $P2_1/n$, with a

† Università di Salerno.
‡ IBM Research Division, Almaden Research Center.
® Abstract published in *Advance ACS Abstracts*, April 1, 1994.

0024-9297/94/2227-3295$04.50/0

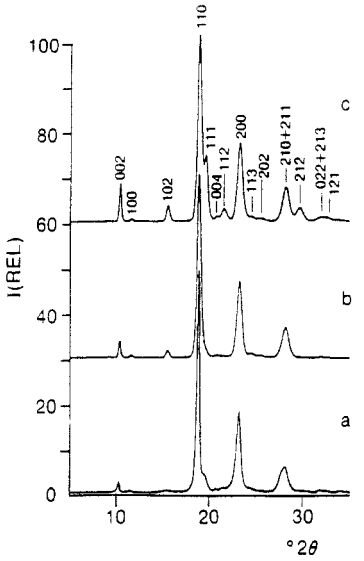

Figure 1. PHNA at room temperature. Comparison between the observed X-ray pattern (a) and the ones calculated by a $Pbc2_1$ space group: (c) case without disorder and (b) case considering *up* and *down* molecule disorder and displacement along the *c* axis (see text).

Table 1. Data for PHNA at Room Temperature (See Figure 1)

				I(calc)	
hkl	2θ(obs)	2θ(calc)	*d*(obs)	up–down	up–up
002	10.30	10.33	8.59	4	11
100	11.44	11.55	7.73	1	1
102	15.48	15.52	5.72	3	7
110	18.86	18.85	4.71	100	100
111	19.52	19.55	4.55	4	35
004	20.64	20.75	4.30	1	2
112	21.54	21.54	4.13	<1	7
200	23.26	23.22	3.82	52	52
113		24.51		2	2
202		25.48		1	2
210	27.66	27.67	3.22	1	1
211	28.12	28.17	3.17	25	27
212		29.61		<1	12
022	31.78	31.75	2.82	1	1
024		36.71		2	2
310	38.48	38.34	2.34	1	1
008	42.52	42.23	2.13	2	3

molecular conformation having staggered phenyls along the chain. For the poly(*p*-benzamide) with a close chemical analogy with PHBA, Hasegawa et al.[14] proposed the orthorhombic space group $P2_12_12_1$ with a screw axis along the chain. Following the example of wholly aromatic main-chain polymers, all peaks in the powder diffraction pattern of PHNA can also be explained using an orthorhombic cell with a = 7.66 (2) Å, b = 5.98 (1) Å, and c = 17.12 (3) Å. The computed volume of 784 (1) Å^3 is consistent with 4 monomer units per unit cell (ρ_{calc} = 1.44 g cm^{-3}). The cell parameters can be compared with those of the analogous orthorhombic PHBA compound in which a = 7.4 Å, b = 5.7 Å, and c = 12.5 Å.[12] In both cases the *c* axis is determined by the two-unit repeat of the polymer chain, which is of course larger for the HNA derivative.

The two monomers along the chain might be related to each other by a symmetry operator that can be either a glide plane or a screw axis. Biswas et al.[11] analyzed the behavior of random copolymers between HNA and HBA in the solid state and described the effect of the two chain conformations corresponding to a screw axis and a glide plane on the X-ray diffraction patterns of fiber samples. They found better agreement between the experimental and computed data using the glide plane. Following this idea and using the extinction conditions, only the space group $Pbc2_1$, which requires the molecular chain to lie on the *c* glide plane, is consistent with good molecular packing in the PHNA case. In this symmetry, the rigid naphthoic rings are staggered along the chain. However, this packing involves edge-face interactions between adjacent molecules. In a recent study[8] on PHBA at room temperature, we found a similar edge-face intermolecular interaction that was still present in the high-temperature phase as reported by previous studies.[6,7] Since the naphthoic rings are quite parallel to the 110 plane, the high electron density gives a strong 110 reflection and a 200 reflection with about half the intensity as can be seen in the experimental data (Figure 1).

Assuming that the chain possesses a screw symmetry, only the space groups with a glide plane or a screw axis along the *b* axis allow edge-face interaction. Therefore, only the space groups $P2_12_12_1$ and $Pbn2_1$ remain to be considered. Because of the extinction conditions, they do not explain the weak 100 peak at 11.44° and, in the $Pbn2_1$ case, also the weak and broad 102 peak at 15.48°. Moreover, a strong inclination of the naphthoic rings is required in order to achieve good molecular packing, and this is incompatible with the observed 110 and 200 intensities.

Because of the small number of reflections, we cannot exclude *a priori* a possible lower symmetry system such as, for example, a rectangular monoclinic cell (γ = 90°). In fact, if the glide plane is omitted, the space group would then be $P2_1$, although this hypothesis removes the extinction condition for the 101 and 010 reflections which are clearly absent in the experimental pattern. In this case the coordinate y_0 of the geometric center of the molecule and its rotation Φ_0 around the chain axis have to be evaluated.

Model Calculation. All calculations were carried out by applying the Rietveld procedure,[15] which analyzes the whole X-ray diffraction pattern from a powder polycrystalline sample. The internal coordinates, such as bond and torsion angles and bond lengths, were employed[16] instead of the atomic fractional coordinates. Because of the noncontinuous trend of the peak widths versus 2θ in the experimental diffraction pattern, we could not fit well any of the peak profiles, and thus it was not possible to refine the molecular structure. Therefore, all the structural parameters defined in Figure 2 and listed in the upper portion of Table 2 were kept constant, and only the torsion angles τ_1 and τ_2 were optimized by a *trial and error* procedure. The torsion angle τ_3 was fixed at 180° because this value well reproduces the repeat unit length. The contribution of hydrogen atoms to the calculated diffraction pattern was also considered, by evaluating the atomic coordinates by means of the canonical sp^2 hybridization geometry. The isotropic thermal parameter B_{iso} = 8 Å^2 was set equal for all the atoms.

Using the space group $Pbc2_1$, the geometric center of the molecule was placed and fixed at the coordinates x_0 = 0.25 and y_0 = 0.25, while the origin on the *z* axis was arbitrarily assigned to the *z* coordinate corresponding to the middle of the esteric bond C–O. y_0 was fixed at 0.25 because of the *c* glide plane, and the x_0 value ensures good molecular packing for geometrical reasons, being in the middle of successive screw axes in the cell. The best match was obtained by staggering the two naphthoic units by ca. 120°. The differences between the observed and calculated diffraction patterns were then mainly due to the 102, 002, 111, and 212 Bragg reflections, whose intensities are

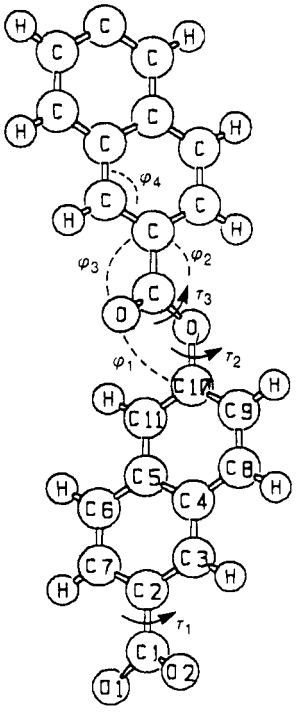

Figure 2. Internal coordinates (angles and atomic bonds) for defining the crystal structure of PHNA. The atomic labeling is also indicated.

Table 2. Structural Parameters Kept Constant during the Molecular Structure Analysis and Optimized Structural Parameters of the Molecular Structure at Room Temperature (RT) and High Temperature (HT) (See Figure 1)

Structural Parameters

bond	length (Å)		angle (deg)
C=C (aromatic)	1.40	$\varphi_1 = \varphi_2$	120
C–O	1.41	φ_3	120
C=O	1.23	φ_4	120
C–C	1.49	τ_3	180
C–H	1.08		

Optimized Structural Parameters

	RT (deg)	HT (deg)
τ_1	160	180
τ_2	108	92

stronger in the calculated than in the experimental pattern (see Figure 1).

Lower intensities can be obtained if an *up* and *down* statistical disorder is considered involving a 2-fold axis perpendicular to the molecular chain, lying in the *c* glide plane and passing through the *z*-position of the center of the ester C–O bond. To check this point, a view of molecular packing is shown in Figure 3. Because of the edge-face interaction and the almost perpendicular arrangement of the naphthoic rings to the *a*–*b* plane, the molecule can be statistically oriented *up* or *down* along the *c* axis, i.e., by a 180° rotation around an axis normal to the chain. This causes smaller 102, 111, and 212 intensities especially for the 111 reflection, whose intensity decreases dramatically (see Table 1 and Figure 1). This can be explained by looking at the naphthoic rings. If no disorder is applied, the naphthoic ring lies almost parallel to the 111 plane, thus strongly contributing to the 111 Bragg reflection. If a disorder is applied, a second naphthoic ring is superimposed to the first one with a less favorable inclination with respect to the 111 plane, thus bringing a weaker reflection. After the statistical model is applied, the calculated 002 peak is still too strong and

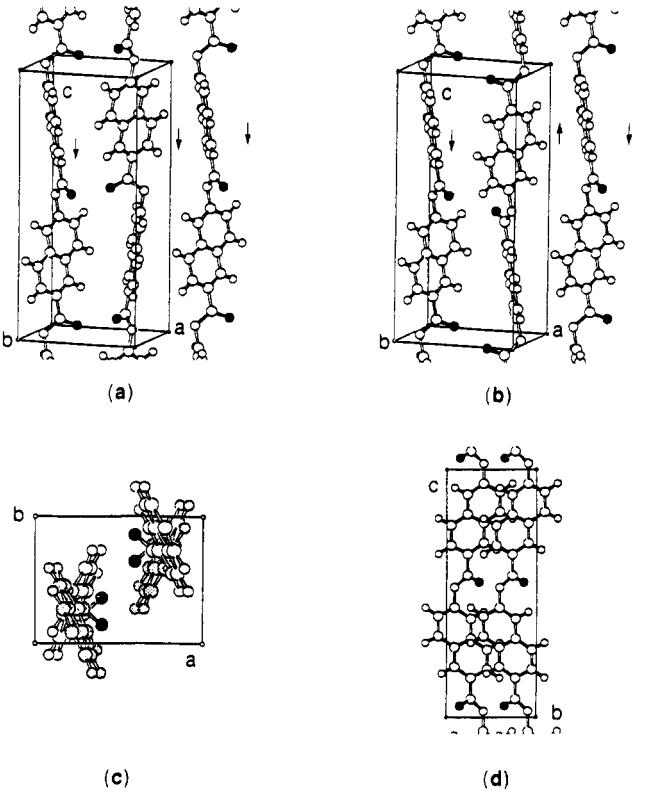

Figure 3. Projection of the PHNA molecular packing on the *a*–*b* plane (c) and *b*–*c* plane (d) at room temperature. Just for the sake of clarity the molecular packing is shown for the *down*–*down* (a) and *up*–*down* (b) statistical arrangement. The *up* and *down* chains are placed in each lattice position with the same occupancy. The carbonyl oxygen atoms are shown by filled circles.

it is not possible to improve the match to the observed one because the intensity depends only on the *z* atomic coordinates that are practically independent of the structural parameters. Only the displacement of molecules along the *c* axis could decrease the 002 intensity. This necessitates shifting the *up* molecule with respect to the *down* one. The best match was obtained by a shift of ca. 1.7 Å which reduced the 002 peak intensity to about that in the experimental pattern (Figure 1b).

According to the above model, the final parameter values and the atomic coordinates are listed in Tables 2 and 5, respectively. The projections of the molecular packing on the *a*–*b* plane and on the *b*–*c* plane are shown in parts c and d of Figure 3, respectively. Checking the intermolecular steric interactions, we found reasonable distances between adjacent atoms with the minimum values 3.24 Å (C–C), 3.27 Å (C–O), and 3.33 Å (O–O), while the values of the τ_1 and τ_2 torsion angles avoid intramolecular interaction between the carbonyl oxygen and the closest hydrogen atom (2.54 Å).

PHNA at High Temperatures. The DSC heating trace of PHNA (Figure 4) shows two transitions at ca. 340 and 440 °C. Consistent with these results, two phase transformations are observed starting at about 330 and 430 °C in the X-ray diffraction pattern. Figure 5 shows the patterns recorded across the first phase transition in agreement with those reported by Kricheldorf *et al.*[4] The transition is complete at 370 °C. At temperatures between 360 and 450 °C, all peaks can still be indexed on the basis of an orthorhombic cell. The temperature dependence of the unit cell parameters is shown in Table 3. The cell parameters were not refined because of the small number of peaks. In PHBA[6,7] there is evidence of a pseudohexagonal or idealized hexagonal symmetry, denoted by the $a = 3^{1/2}b$ relation of the lattice parameters of the high-

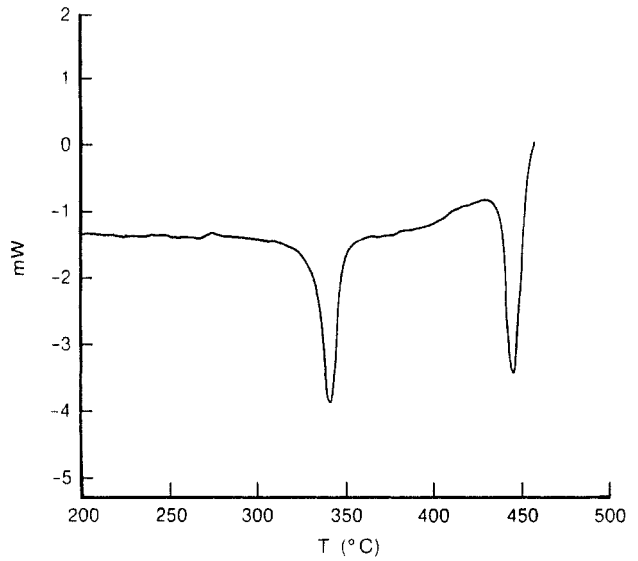

Figure 4. DSC trace of PHNA as received at a heating rate of 10 °C/min.

temperature phase. In the present case, the a/b ratio approaches this value when the temperature is increased but the 211 reflection persists; hence, it cannot be hexagonal.

Heating of the sample to higher temperatures across the phase transition starting at about 430 °C resulted in a progressive decrease of the intensities of all the peaks consistent with the loss of the three-dimensional order in the packing. Figure 6 shows the patterns recorded from

Table 3. Temperature Dependence of the Lattice Parameters of PHNA[a]

T (°C)	a (Å)	b (Å)	c (Å)	V (Å^3)
25	7.66 (1)	5.98 (1)	17.12 (3)	784 (1)
215	7.84 (1)	6.02 (1)	16.99 (1)	802 (1)
325	8.03 (1)	5.99 (1)	16.95 (3)	815 (1)
370	9.28	5.64	17.04	892
430	9.46	5.59	17.00	899
440	9.50	5.60	17.00	904
450	9.51	5.61	16.99	906

[a] The standard deviations at high temperature are not reported because of the small number of diffraction peaks.

410 to 480 °C, at 10 °C steps. At about 480 °C the pattern shows only a broad amorphouslike peak centered at about 17° 2θ. Slow cooling of the sample to room temperature over a period of about 3 h did not restore any of the crystalline or liquid crystalline phases; partial decomposition of the polymeric material had occurred, as was also determined by thermal gravimetric analysis. Therefore, no conclusion on phase transition can be drawn from our measurements.

The structure analysis was begun using the same space group $Pbc2_1$ found at room temperature and adjusting the cell parameters. The cell is larger than that of the room temperature phase (Table 3), thus allowing more space for molecular mobility in the packing. We assume statistical *rotational disorder* as represented by a 2-fold symmetry axis along the chain, which is similar to that found in the PHBA phase at high temperature.[6,7] In crystallographic notation, this corresponds a change of

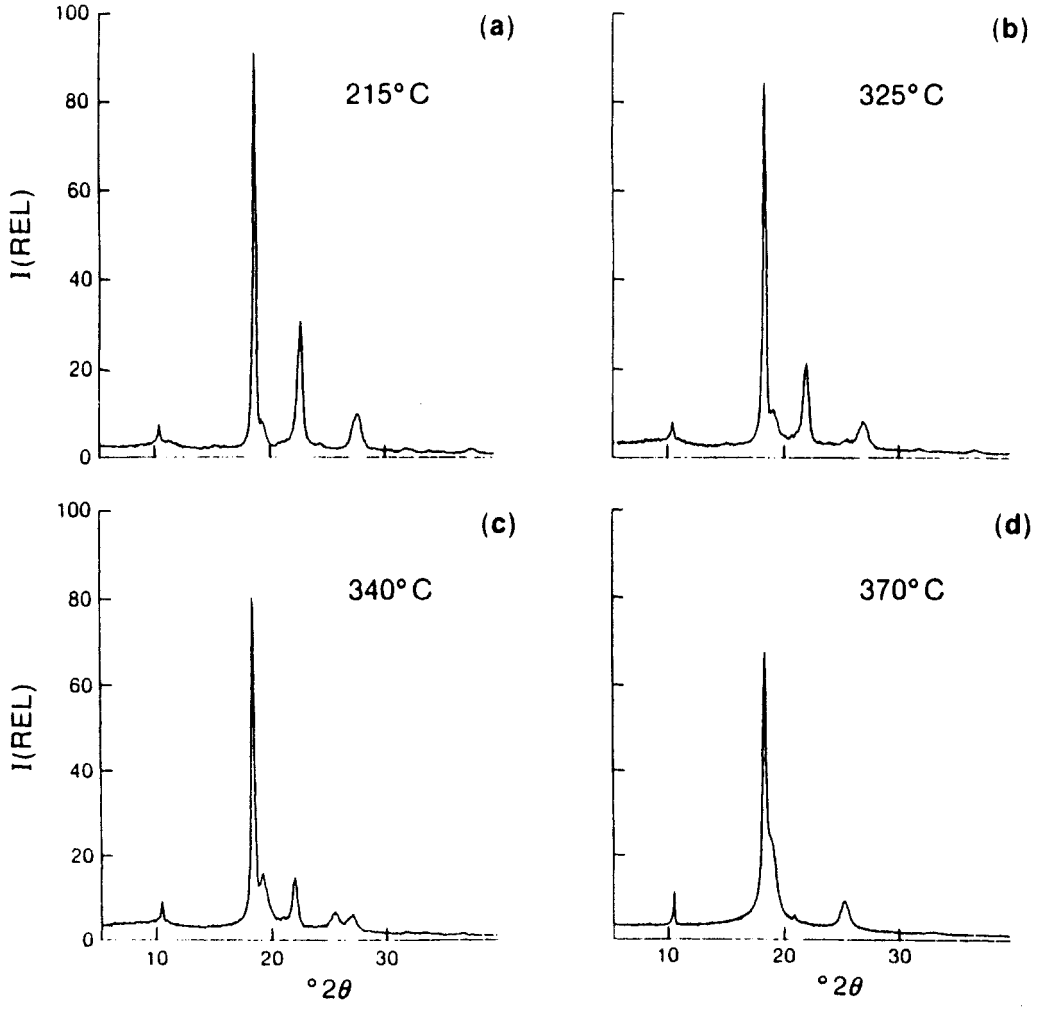

Figure 5. Observed X-ray diffraction pattern for PHNA at four different temperatures: (a) 215, (b) 325, (c) 340, and (d) 370 °C.

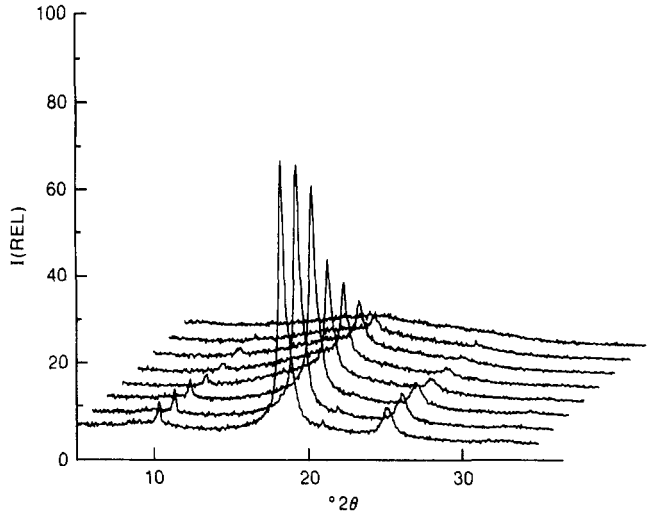

Figure 6. Observed X-ray diffraction pattern for PHNA during heating across the second phase transition.

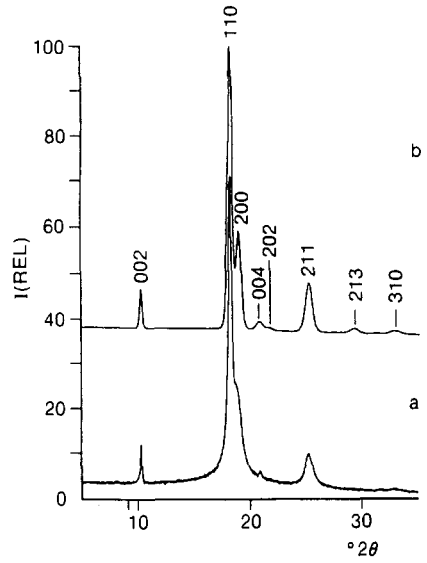

Figure 7. PHNA at 370 °C. Comparison between the observed X-ray pattern (a) and the calculated one (b) with *up* and *down* statistic.

the space group from $Pbc2_1$ to $Iba2$ and a move of the geometrical center of the molecule to the cell origin (x_0 = 0.0; y_0 = 0.0).

We think that the hypothesis of only one conformer in the cell is arbitrary and its statistical replacement by the 2-fold axes is only an averaged representation of the true molecular packing. We believe that different conformers are present at the same time because of the available space and the low conformational energy,[17] thus allowing the torsion angles τ_1 and τ_2 to vary. For the same reason the symmetry operators such as the *c* glide plane reproduce only the averaged symmetry in the cell. Consequently, we arbitrarily fixed τ_1 at 180°, placing the carbonyl group in the naphthoic plane.

Optimizing the structure in the same way as we did for the room-temperature one but without imposing the shift between the *up* and *down* molecules, we obtained good agreement between calculated and observed patterns as shown in Figure 7b. The final τ_2 value, corresponding to a higher angle between the staggered naphthoic rings along the chain compared to the room-temperature case, leads to the new *c* axis. The X-ray diffraction data are reported in Table 4, and the structural parameters are listed in Table 2. The atomic coordinates are given in Table 5. Figure 8 shows the equatorial projection of the molecular

Table 4. Data for PHNA at 370 °C (See Figure 9)[a]

hkl	2θ(obs)	2θ(calc)	*d*(obs)	*I*(calc)
002	10.38	10.38	8.52	8
110	18.34	18.34	4.84	100
200	19.08	19.13	4.65	32
004	20.95	20.85	4.24	1
202		21.81		1
211	25.36	25.35	3.51	23
310	32.90	32.98	2.72	2
008	42.75	42.44	2.12	1

[a] The calculated integrated intensity *I*(cal) is given for each reflection.

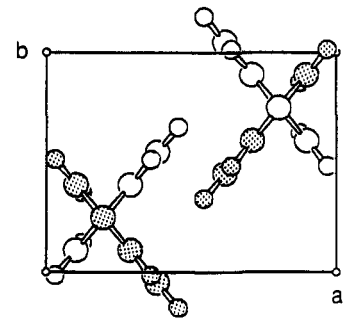

Figure 8. Projection of the PHNA molecular packing on the *a*–*b* plane at 370 °C.

Table 5. Atomic Fractional Coordinates for PHNA at Room Temperature (RT) and at High Temperature (HT)

	RT			HT		
	x	*y*	*z*	*x*	*y*	*z*
O1	0.193	0.089	0.026	0.196	0.250	−0.021
O2	0.403	0.355	0.047	0.373	−0.031	−0.015
C1	0.291	0.231	0.075	0.290	0.100	0.021
C2	0.260	0.231	0.160	0.290	0.100	0.108
C3	0.312	0.411	0.205	0.197	0.250	0.149
C4	0.282	0.411	0.285	0.197	0.250	0.231
C5	0.201	0.231	0.320	0.290	0.100	0.273
C6	0.148	0.051	0.275	0.384	−0.049	0.231
C7	0.178	0.050	0.195	0.384	−0.049	0.149
C8	0.334	0.592	0.329	0.103	0.399	0.273
C9	0.305	0.592	0.409	0.103	0.399	0.355
C10	0.223	0.411	0.444	0.196	0.250	0.396
C11	0.171	0.231	0.399	0.290	0.100	0.355

packing; for the sake of clarity only one molecule of the statistical model is shown. It is evident that the molecules are related to each other along the *z*-direction because of the interaction of the staggered naphthoic rings.

Conclusion

We have shown that the molecular packing of PHNA at room temperature involves the face-edge interaction which is a recurrent feature of this class of aromatic materials. The conformational model of the chain, with the two naphthoic rings staggered by ca. 120° along the chain axis, is retained in the high-temperature phase and the naphthoic rings have no free rotation around their center of mass. Because of the tight packing, they are registered to give a layered three-dimensional structure, similar to that reported for PHBA.

Acknowledgment. P.I. is indebted to IBM Italy for granting a visiting scientist fellowship.

References and Notes

(1) Calundann, G. W. (Celanese Corp.). U.S. Patent 4,395,513, July, 26, 1983.

(2) Cao, M. Y.; Wunderlich, B. J. *J. Polym. Sci., Polym. Phys. Ed.* **1985**, *23*, 521.
(3) Muhlebach, A.; Lyerla, J.; Economy, J. *Macromolecules* **1989**, *22*, 3741.
(4) Schwarz, G.; Kricheldorf, M. R. *Macromolecules* **1991**, *24*, 2829.
(5) Economy, J.; Volksen, W.; Viney, C.; Geiss, R.; Siemens, R.; Karis, T. *Macromolecules* **1988**, *21*, 2777.
(6) Yoon, D. Y.; Masciocchi, N.; Depero, L. E.; Viney, C.; Parrish, W. *Macromolecules* **1990**, *23*, 1793.
(7) Coulter, P. D.; Hanna, S.; Windle, A. H. *Liq. Cryst.* **1989**, *5*, 1603.
(8) Iannelli, P.; Yoon, D. Y.; Parrish, W. *Structures of Poly(p-hydroxybenzoic acid) (PHBA) at Ambient Temperature, J. Polym. Sci., Phys. Ed.*, in press.
(9) Parrish, W. *X-ray Analysis Papers*; Centrex Publishing Co.: Eindhoven, The Netherlands, 1965.
(10) Huang, T. C.; Parrish, W. *Advances in X-Ray Analysis*; Plenum Press: New York, 1984; Vol. 27, p 45.
(11) Biswas, A.; Blackwell, J. *Macromolecules* **1988**, *21*, 3152.
(12) Lieser, G. *J. Polym. Sci., Polym. Phys. Ed.* **1983**, *21*, 1611.
(13) Northolt, M. G. *Eur. Polym. J.* **1974**, *10*, 799.
(14) Hasegawa, R. K.; Chatani, Y.; Tadokoro, H. Meeting of the Crystallographic Society of Japan, Osaka, Japan, 1973.
(15) Rietveld, H. M. *Acta Crystallogr.* **1967**, *22*, 151.
(16) Arnott, S.; Wonacott, J. *Polymer* **1966**, *7*, 157.
(17) Jaffe, X. L.; Yoon, D. Y.; McLean, A. D. *The computer simulation of polymers*; Prentice Hall: New George, 1991; p 1.